Repeated nutrient, oxygen, and density sections through the Loop Current

by John M. Morrison[1] and Worth D. Nowlin, Jr.[1]

ABSTRACT

Based on observations made in May, 1972, the nutrient and dissolved-oxygen concentrations in the offshore waters of the eastern Gulf of Mexico are described and related to the Loop Current and anticyclonic current rings, which are the principal circulation features of this region. The characteristic relationships of oxygen and nutrients to density parameters are presented, and the following water masses are characterized in the Gulf: Subtropical Underwater, 18°C Sargasso Sea Water, upper subtropical oxygen minimum, Antarctic Intermediate Water, and North Atlantic Deep Water.

Repeated sections through the Loop Current allow some estimation of variability within a period of weeks, as well as descriptions of spatial variations of properties. The relative geostrophic flow within the Loop is described. Transport estimates are compared to previous estimates of the Loop and to estimates through the Yucatan and Florida Straits based on measurements also made during May, 1972. The results are in good agreement: values for the total transport of the current are approximately $30 \times 10^6 m^3 sec^{-1}$, while for the waters above σ_t = 27.0 mg cm^{-3} a value near $23 \times 10^6 m^3 sec^{-1}$ is obtained.

1. Introduction

The major circulation features of the eastern Gulf of Mexico are the Loop Current (comprised of the Yucatan Current and its downstream extension through the Gulf and into the Straits of Florida) and the anticyclonic current rings which separate from this Current. These features are among the principal potential sources of energy for driving the mesoscale circulation of the entire Gulf of Mexico. Of considerable interest, therefore, are specific relationships of water characteristics, including dissolved oxygen and nutrients, to the Loop Current and rings. Although the occurrence and configuration of the Loop Current and such rings cannot yet be predicted, they are easily detected by measurements of salinity and temperature. Knowledge of how the nonconservative properties are related to these current features should be useful in determining property distributions throughout the offshore water of the Gulf.

1. Department of Oceanography, Texas A&M University, College Station, Texas, 77843, U.S.A.

In 1959, Wennekens reviewed the distribution of properties in the eastern Gulf of Mexico and its Straits. He related the concentrations of dissolved oxygen and phosphate-phosphorous to water density in an attempt to differentiate systematically water types, their sources, and local modifications thereto. At that time the data base was exceedingly small, e.g., Wennekens had data from only two cruises from which to characterize dissolved-oxygen concentrations within the eastern Gulf. Moreover, many of the data were of poor quality, as Wennekens pointed out in the case of phosphate values.

The distribution of dissolved oxygen below sill depth in the Gulf of Mexico has been described by Nowlin, Paskausky, and McLellan (1969). Study of data from ten cruises suggested no clearly discernible horizontal variation, only a slight vertical increase of dissolved oxygen with depth below 1500 m, and a mean value within the Gulf of Mexico Basin waters of approximately 5.0 ml l^{-1}.

Based on a 1962 winter survey of the entire Gulf, Nowlin and McLellan (1967) described the general distribution of dissolved oxygen together with temperature and salinity distributions. Although the major features were recognized and vertical profiles were presented to characterize the distinct oxygen-depth relationships found on opposite sides of the Loop Current, detailed relationships of dissolved-oxygen concentration to current structure or to other parameters could not be determined because of the coarse grid used in the 1962 survey.

A summary of the status of chemical oceanographic knowledge of the eastern Gulf of Mexico was prepared in 1973 by Corcoran. Included were brief reviews of published works on distributions of oxygen and phosphate. The work of Riley (1937) showed that the Mississippi River increased near-surface phosphorous concentrations in the vicinity of its mouth. As Corcoran (1973) pointed out, that work has been extended by several workers, but mainly in areas near shore.

Regarding the offshore waters, Wennekens (1959) was unable to make any generalizations concerning the relation of phosphate to water masses in the eastern Gulf because of the "scarcity and unreliability of the available data." In 1968, Paskausky and Nowlin portrayed the vertical distributions of measured and preformed phosphate as observed on three cruises which covered the deep water regions of the Gulf of Mexico. Scatter in the data was great, and consequently only the characteristic regional distribution was discussed. The phosphate characteristics of the Subtropical Underwater, Antarctic Intermediate Water, and North Atlantic Deep Water were identified, and the relationship of oxygen to phosphate concentrations was briefly discussed.

Many unpublished data and technical reports give dissolved-oxygen and phosphate-phosphorous concentrations for the Gulf of Mexico, but little has been published on the subject. Most of these data were collected over continental shelves or as peripheral information on cruises for distinctly different purposes.

In May of 1972, we collected oceanographic station data from the regime of the

Loop Current in the eastern Gulf of Mexico. Measured variables included dissolved-oxygen concentration, concentrations of the dissolved nutrients, silicate and phosphate, and the traditional parameters, temperature and salinity, as functions of pressure. Three sections of stations across the Yucatan Current, two of which were occupied several times, provided an unusual suite of data for study. The results of that field work are presented in this paper with two distinct objectives.

Our first objective is to document the observations of dissolved oxygen and nutrients in the Loop Current and their relation to distributions of density parameters and relative geostrophic speeds. This information is presented mainly in vertical sections across the Yucatan Current and its downstream extension. The mesoscale circulation and offshore property distributions in the Gulf seem dominated by the Loop Current and anticyclonic rings which detach from it. Therefore, the relationships of dissolved oxygen and nutrient distributions to this Current should enable one to infer nutrient distributions in the eastern Gulf from specific information on the current distributions.

The second objective is to indicate the variability observed during the interval of several weeks in which observations were repeated. The spatial variability of volume transport and property distributions along the Yucatan Current may be assessed by comparing cross-stream sections occupied at distinct positions.

The observations were made on R. V. *Alaminos* cruise 72-A-9, part of a CICAR (Cooperative Investigations of the Caribbean and Adjacent Regions) field effort involving ships and aircraft from Nova University, the Atlantic Oceanographic and Meteorological Laboratories of NOAA, the State University System Institute of Oceanography, Florida, the Universidad National Autonama de Mexico, and Texas A&M University. The overall purpose was to describe the Loop Current during May and to relate its variability to measurements of hydrographic and kinematic variables at the Yucatan Strait and the Florida Straits. Selected bathythermograph observations made aboard the R. V. *Bellows* were used together with R. V. *Alaminos* data to describe the topography of the 22°C isothermal surface.

Data collection aboard *Alaminos* was by expendable bathythermograph (XBT) and a salinity-temperature-depth sensor (STD) with a rosette sampler. Twelve water samples and three values of *in situ* temperature and thermometric depth were obtained at each STD sation. For all water samples, salinities were determined abroad ship using an inductive laboratory salinometer. Bottle salinities, temperatures, and depths were used to standardize or verify the STD values. All water samples were analyzed for concentrations of dissolved silicate, phosphate, and nitrate-nitrite using the procedures described by Atlas *et al.* (1971) and a Technicon Basic Analyzer. Not all analyses could be completed aboard ship; frozen samples were stored for post-cruise analysis for nitrate-nitrite concentrations. Apparently these samples were ruined in storage or handling, because replicate analyses showed gross differences. Thus, no nitrate-nitrite values were reported or used.

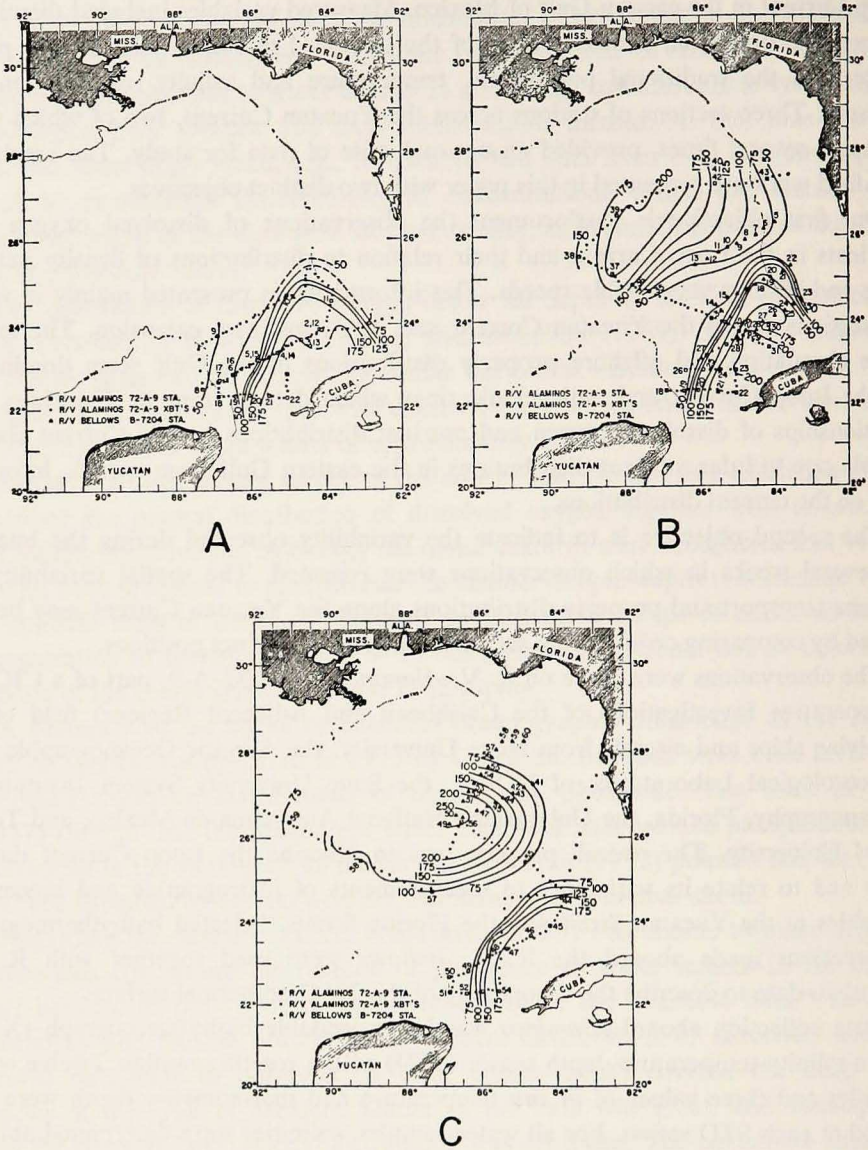

Figure 1. Depth (m) of the 22°C isothermal surface constructed using data from *Alaminos* 72-A-9 and *Bellows* B-7204. Positions and numbers of stations and bathythermographs are shown.

a. For stations 1-23 of 72-A-9, 2-8 May 1972.
b. For stations 18-43 of 72-A-9 and 5-30 of B-7204, 7-13 May 1972.
c. For stations 44-59 of 72-A-9 and 41-60 of B-7204, 16-21 May 1972.

A complete listing of data from *Alaminos* 72-A-9 is available in an unpublished report (Ref. 73-10T) of the Department of Oceanography, Texas A&M University,

by Morrison, Merrell, and Nowlin (1973). Also included in that report are details of the data collection and correction procedures as well as estimates of accuracy and precision.

2. Property distributions in sections

Current patterns in the eastern Gulf of Mexico at the time these data were collected may be inferred from Figs. 1a, b, and c, which show the regional topography of the 22°C isothermal surface. It has been shown repeatedly that the topography of any isothermal surface between about 10° and 22°C is an excellent indicator of the geostrophic current regime in this region. From these figures it is seen that the Loop Current extended not far into the central eastern Gulf. An anticyclonic ring had only recently separated from that Current and was situated approximately over the center of the eastern Gulf. An upper limit on the age of the ring can be placed at one month, based on observations by Morrison during a prior *Alaminos* cruise (72-A-7). Those observations indicate that, during 25-27 March, 1972, the Loop Current extended well into the Gulf and no ring was present in the eastern Gulf.

Because of the repetitive nature of the cruise track, we chose to contour depth patterns for the 22°C isothermal surface for three different time periods. The Loop Current is seen to have extended slightly less far to the north during the third time period (Fig. 1c) than during the first two periods. That portion of the separated ring which was observed appears to have become more symmetrical between the times of the second and third patterns shown.

The locations of both oceanographic stations and expendable thermographs are shown in Fig. 1. Both Omega and satellite navigation receivers were used for navigation; positions are considered accurate to well within 5 km. Characteristics on three vertical sections will be considered. These sections, referred to as A, B, and C, are located along the lines of *Alaminos* stations 18 through 22, 23 through 26, and 26 through 30, respectively, as seen in Fig. 1b or 12.

In Fig. 2 are presented vertical profiles of salinity, dissolved oxygen, silicate, and phosphate concentrations at four stations located on Section C at positions (see Fig. 1a) spanning the Loop Current. The times of crossings 1, 2, 3, and 4 of Section C are, respectively, May 2-4, May 6-7, May 8-9, and May 16-17. The strong salinity maximum near 200 m depth at Station 3 is typical of the Subtropical Underwater core as found in the central Cayman Sea south of Yucatan Strait. This water is sometimes called Caribbean-type (or Loop water) to distinguish it from the Gulf-type water which is found in the Gulf to the left-hand side of the Loop Current and outside the anticyclonic rings. As compared with the Carribbean-type water, this Gulf-type water has a considerably different temperature-salinity relation for temperature greater than 16°C, with distinctly lower salinity values at the Subtropical Underwater core.

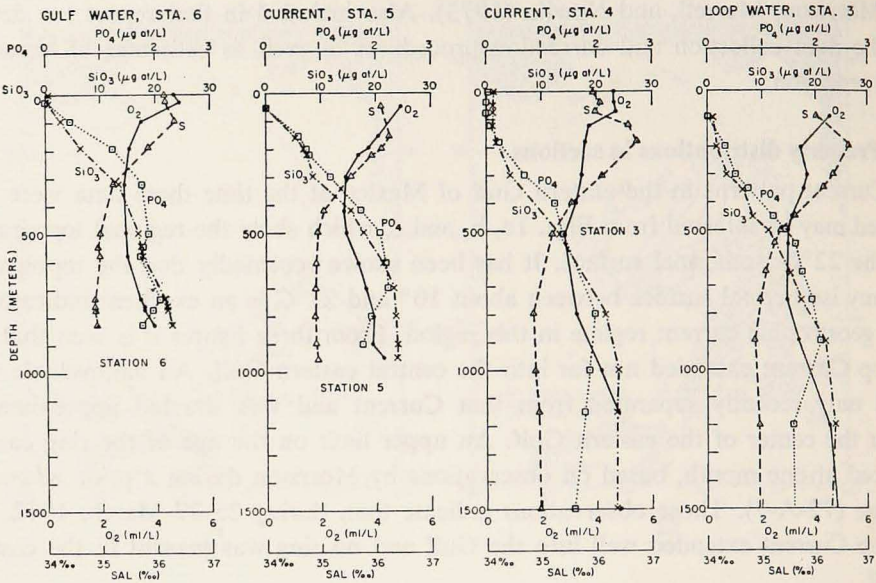

Figure 2. Vertical profiles of salinity, dissolved-oxygen, dissolved-phosphate, and dissolved-silicate concentrations at stations positioned across the Loop Current.

In Figs. 3-7 are shown vertical sections of temperature, salinity, dissolved oxygen, silicate, and phosphate from the four distinct crossings of Section C. To aid in the discussions, the position of Station 7 has been used as a reference point, and distance in kilometers from that point is shown along each section. Also shown, superimposed on the property distributions, for each crossing are isotachs of geostrophic speed normal to the section.

The geostrophic speeds were referenced to the pressure at the deepest observation taken on the particular section. At stations for which the deepest sampling depth or the bottom depth was less than this reference, extrapolation of the geopotential anomaly to the reference pressure was done using a method devised by R. O. Reid and R. Schlitz (Schlitz, 1973). Using this method the specific volume anomaly at a shallow station is extrapolated in depth from the value at the deepest observed level to the value at the deepest observed level for the adjacent deeper station. If the reference level lies below the deepest observation level of the adjacent deeper station, the specific volume anomalies used for those deeper levels at the shallower station are just those which have been obtained in a similar manner by extrapolation for the adjacent deeper station. All such extrapolated specific volume anomalies are then used, together with the observed anomalies, to compute geopotential anomalies down to the common reference level for a section. Procedures for extrapolating geopotential anomalies in depth when water depth is shallower than the desired reference level, or when observations at depth are missing, are numerous

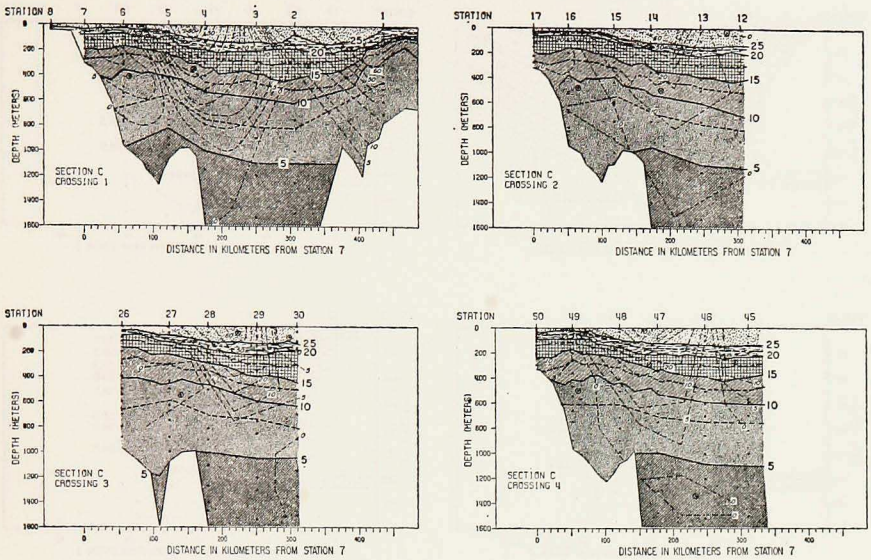

Figure 3. Vertical sections of temperature (°C) for the 4 crossings of Section C. Superimposed are isotachs of relative geostrophic speed (cm sec^{-1}) normal to the section.

in the literature, of course; see Fomin (1964). The novel aspect of the Reid and Schlitz scheme lies in the method by which such extrapolation is carried out. Specific volume is extrapolated by an algorithm which specifies that the horizontal gradient of pressure, and therefore the geostrophic current, vanishes at the bottom, or at the deepest observable level if less than the bottom, and that there is zero flow below this surface.

The geostrophic speeds at the core of the inflowing limb of the Loop Current, namely, the Yucatan Current, are seen to have the same general pattern in all four crossings. The maximum speeds observed near the surface are greater than 60 cm sec^{-1}; they reach values larger than 80 cm sec^{-1} in crossing 1. Speeds of 10 cm sec^{-1} extend to depths of nearly 700 m in all crossings. The lateral extent of the current having speeds greater than 10 cm sec^{-1} normal to this section is approximately 200 km in each section. The current core seems slightly sheared with depth so that maximum speeds in the northward flow are found farther to the east at greater depths within the water column. It should be remembered that Section C is not normal to the axis of the current. (See Fig. 1.) Therefore, the relative geostrophic speeds shown in these sections are less than the maximum relative geostrophic speeds in the direction of the current axis.

Some temporal variability of the property distributions and current structure may be seen by comparing the four separate crossings of Section C (Figs. 3-7) made during the three-week observation period. Relative to its position at the time of crossing 1, the northward flowing current seems to have shifted its axis somewhat

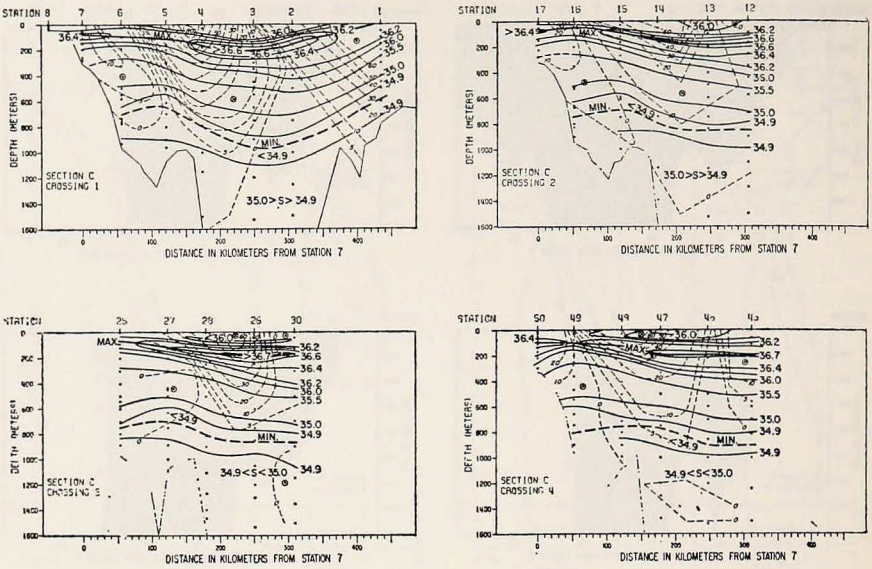

Figure 4. Vertical sections of salinity (‰) for the 4 crossings of Section C. Superimposed are isotachs of relative geostrophic speed (cm sec^{-1}) normal to the section.

to the east by the times of crossings 2 and 3. During the period between crossings 3 and 4 the current axis seems to have again shifted westward. In crossing 2 none of the southeastward flowing limb of the Loop Current is evidenced. A slight southward flow is seen at the eastern end near the surface in crossing 3. Then in crossing 4, after a westward shift of the current axes, southward flow is seen over an extent of approximately 75 km at the eastern end of the section. Crossing 1, which extends considerably farther to the east than do the other three crossings, clearly shows the edge of the major southeastward flow.

The maximum geostrophic speeds in the Yucatan Current were observed to be larger when the current was situated farther to the west (i.e., on crossings 1 and 4) than otherwise. A positive correlation between large geostrophic current speeds and westward position of the Yucatan Current axis was noted for seasonal variations by Cochrane as early as 1963. A difference of approximately 20 cm sec^{-1} was observed in the surface current at the core. In part, this variability may be an artifact resulting from a change in position between successive crossings of the current core relative to the station positions. Such changes might result from current meandering. Indeed, lateral motions of the current were observed farther to the south in the Yucatan Strait by Molinari (1973, personal communication) during the time of the observations. Such motions could be due to the effects of bottom topography upon the current (Molinari, 1967).

To the west of the northward flowing Yucatan Current the isotherms and isohalines slope downward toward the west. This results in southward geostrophic

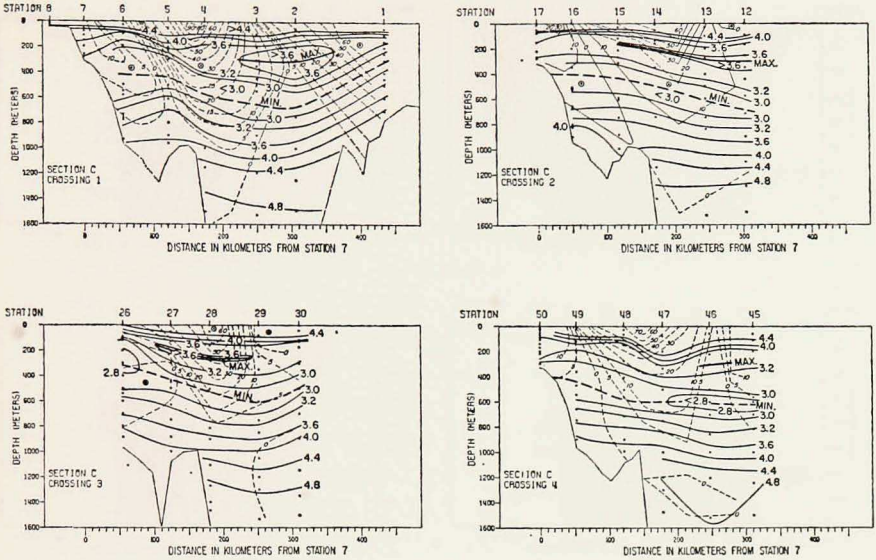

Figure 5. Vertical sections of dissolved-oxygen concentrations (ml l^{-1}) for the 4 crossings of Section C. Superimposed are isotachs of relative geostrophic speed (cm sec^{-1}) normal to the section.

flow if the reference level is taken beneath the level of interest. Referencing the geostrophic speeds to the deepest observation level as we have done results in weak southerly flow (10 cm sec^{-1} maximum) normal to the sections. Cochrane (1969) observed southerly flow in this region. He stated that the observed flow was caused by a cyclonic eddy situated over the edge of the continental shelf of the Campeche Bank. This southward flow is seen in all four crossings of Section C, although in crossing 3 it appears only as a weak subsurface flow in the speed fields. This countercurrent seems stronger when the axis of the northward flowing Yucatan Current was situated farther to the west.

Beneath a well-mixed surface layer of 50 m or less the temperature values (Fig. 3) decrease monotonically with depth to values near 4.25°C at 1600 m, which is within a few hundred meters of the estimated sill depth of the Yucatan Strait connecting the Gulf of Mexico with the Cayman Sea. As already mentioned, the temperature field is a good indicator of currents in this region, with strong temperature gradients indicating the cores of major currents flowing through these sections.

The salinity structure (Fig. 4) is more complex than the thermal structure. The most pronounced feature of the salinity field is the salinity maximum of the Subtropical Underwater. This maximum, which occurs at depths of 150-250 m, has extreme values of 36.70-36.80‰. The maximum values are in the Caribbean-type water found between the northward and southward flowing limbs of the Loop Current in this section. The waters outside of the Loop Current and rings which break

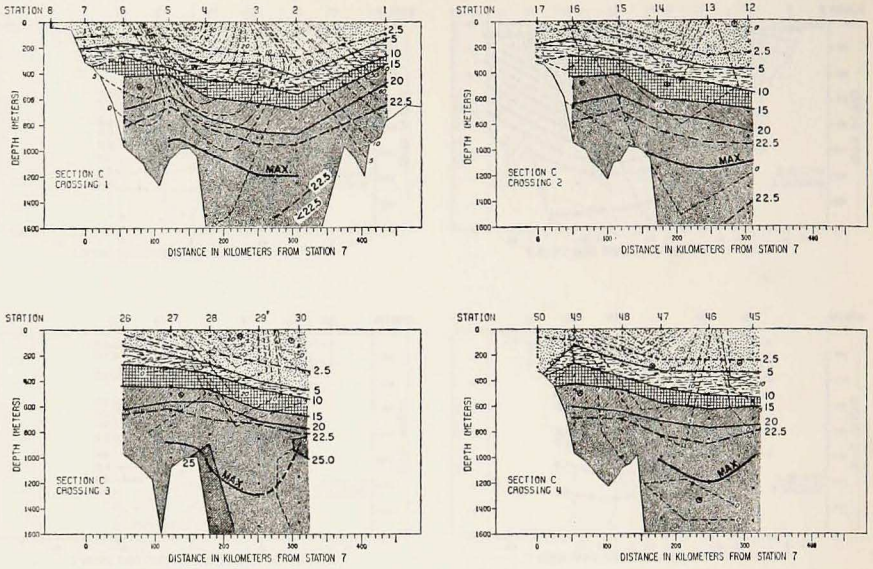

Figure 6. Vertical sections of dissolved-silicate concentration (μg-at l^{-1}) for the 4 crossings of Section C. Superimposed are isotachs of relative geostrophic speed (cm sec^{-1}) normal to the section.

off and are composed of water from that current are referred to as Gulf-type in which salinity values at the Subtropical Underwater core reach only 36.40-36.45‰.

Another definite feature of the salinity field is the minimum associated with Antarctic Intermediate Water, which is found at depths of 800 to 1000 m with values of 34.84-34.88‰ throughout this region. Salinity increases with increasing depth below the core of the Antarctic Intermediate Water, reaching values of approximately 34.97‰ at sill depth.

Above the Subtropical Underwater core, salinities in the surface layer are characteristically less than 36.5‰, but greater than 36.0‰. The vertical sections of salinity show the existence of surface or near-surface pockets of low salinity water (less than 36.0‰), which appear to be derived from low salinity surface waters found in the Caribbean Sea during winter. According to Wüst (1964, plate III) the average salinity values of surface waters in the Cayman Sea during December to May range from just less than 35.5‰ to 36.2‰. The low salinity surface values observed were in the waters bounded by the Loop Current. Tracing these low salinity pockets laterally it was noted that they sometimes have no surface expression, but instead appear only as subsurface salinity minima.

The vertical sections of dissolved oxygen concentration, with superimposed isotachs of relative geostrophic speeds, for the four crossings of Section C are presented in Fig. 5. The most pronounced feature of these sections is a continuous intermediate layer of minimum dissolved-oxygen content. This oxygen minimum

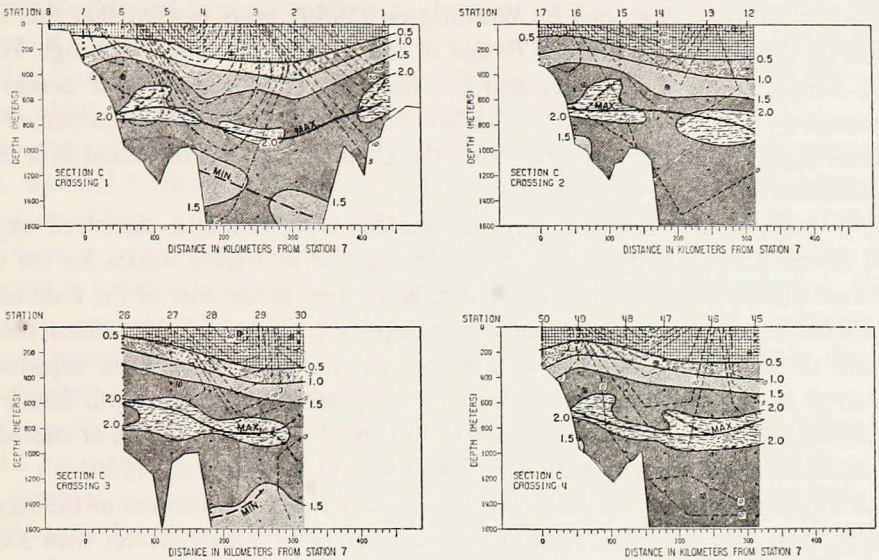

Figure 7. Vertical sections of dissolved-phosphate concentration (μg-at l^{-1}) for the 4 crossings of Section C. Superimposed are isotachs of relative geostrophic speed (cm sec^{-1}) normal to the section.

has been traced throughout the Caribbean Sea by Wüst (1964). The depth variation of this minimum clearly reflects the mass adjustments associated with the currents. The core of the minimum varies from about 650 m in the center of the loop to 400 m outside the Loop Current regime. In the countercurrent to the west of the Yucatan Current the core depth increases westward to intersect the bottom. Crossing 1 shows extreme minimum oxygen values of 2.84 to 2.95 ml l^{-1}. These minimum values are consistent with those of Wüst and Nowlin and McLellan for this region. All the sections of dissolved oxygen examined have minimum values less than 3.0 ml l^{-1}.

A relative oxygen maximum exists within the main oxygen minimum in those waters bounded by the Loop Current. This maximum is clearly seen in individual curves of oxygen versus depth (e.g., Fig. 2) as well as in the vertical sections. In particular, the curves in the Caribbean-type water (within the Loop Current) display two oxygen minima with depth; while in the Gulf-type water outside of the current regime only a single minimum is observed. This suggests that oxygen may be used to indicate the specific water types present. Nowlin and McLellan present typical oxygen-depth curves for this area, which also seem to suggest this difference between oxygen distributions for Caribbean-type waters and Gulf-type waters. The Caribbean-type water in these sections was associated with the reversal or inflection in the oxygen profiles temperatures near 17.3°C and salinities near 36.3‰. These properties identify this water mass with a relative oxygen maximum as the 18°C

Sargasso Sea Water described by Worthington (1959), who showed that this mass enters the Yucatan and Cayman Basins of the western Caribbean through Windward Passage. This water mass also has been identified along 67°W across the Venezuelan Basin by Kinard *et al.* (1974). The occurrence and distribution of this relative oxygen maximum feature within the Caribbean Sea is discussed in a thesis by Morrison (1974).

Above the oxygen-minimum layer the surface layer is rich in dissolved oxygen with values of 4.0 to 5.0 m*l* l^{-1}. These are near the saturation values for the temperature and salinity ranges of the surface layer. Just to the east of the core of the northward flowing Yucatan Current the surface layer appears to be thicker than in the rest of the section, as might be expected from a geostrophic mass adjustment. Dissolved oxygen values decrease monotonically with increasing depth below the intermediate oxygen minimum down to the accepted sill depth. Values at and below sill depth are approximately 4.91 m*l* l^{-1} according to Nowlin *et al.* (1969).

All four crossings of Section C show essentially the same features in the oxygen distributions. The relative oxygen maximum layer (with values greater than 3.6 m*l* l^{-1}) is less pronounced in crossing 4, which is attributed to inadequate bottle spacing between 200 and 550 m at Stations 45 and 46. Each feature seems to occupy the same relative position in the current regime, with the greatest isopleth slopes indicating the current core.

Comparing vertical sections of dissolved oxygen (Fig. 5) with those of salinity (Fig. 4) and of temperature (Fig. 3) shows that the main oxygen minimum lies above the salinity minimum core of the Antarctic Intermediate Water, and just below the remnant core of 18°C Sargasso Sea Water, which is represented by a slight relative subsurface oxygen maximum. In the waters of Gulf-type, outside of the Loop Current regime or anticyclonic rings, no signature of 18°C Sargasso Sea Water is seen; only one relative minimum of dissolved oxygen concentration is seen between the surface layer and the Antarctic Intermediate Water.

The vertical sections of dissolved-silicate concentration along Section C are shown in Fig. 6. Values of silicate are characteristically small near the surface, ranging from 0 to 2 μg-at l^{-1}. This silicate-deficient layer is about 100 m thick outside of the current regime and reaches a maximum thickness of about 200 m in the center of the water bounded by the Loop Current. Dissolved-silicate concentrations remain small through the Subtropical Underwater. At depths of 200 to 400 m, in the main halocline, dissolved silicate concentrations begin to increase rapidly with increasing depth. This trend continues to a depth of about 900 to 1200 m (depending upon position in the current), where concentrations reach a maximum of 23 to 25 μg-at l^{-1}. Below that depth there is a slight decrease in silicate to the greatest observed depth. Although this decrease is not shown in the vertical sections because of their contour interval, it is seen clearly in the vertical profiles of silicate in Fig. 2. Isopleths of dissolved silicate concentration conform very closely to iso-

therms constructed from data taken at the same spatial sampling intervals. Thus, silicate is a sensitive indicator of the mesoscale circulation in this area. It does not exhibit, however, some of the small variations in the water masses of the upper layers which are reflected in the distributions of dissolved oxygen.

Another possible water mass and flow indicator is dissolved-phosphate concentration. Vertical sections of phosphate, upon which isotachs of relative geostrophic speed have been superimposed, are presented in Fig. 7. Clearly, the phosphate distributions in the four crossings of Section C show much more variation from crossing to crossing than do the distributions of other properties presented. Moreover, the spatial distributions of this nonconservative element are configured less like the distributions of the conservative elements temperature and salinity than are the distributions of oxygen and silicate.

The sections in Fig. 7 show a phosphate-deficient surface layer with values of 0 to 0.1 μg-at l^{-1}. Below this layer values increase to maxima of 1.8 to 2.5 μg-at l^{-1}, the depth of which varies from about 600 to 700 m outside of the current to 800 to 900 m in the waters of Caribbean-type. The core of the phosphate maximum lies below the oxygen-minimum layer, but slightly above or at the same level as the salinity minimum associated with Antarctic Intermediate Water. As concluded by Redfield *et al.* (1963), who studied the origin of this maximum, it is probably associated with the remnant of Antarctic Intermediate Water as modified by net phosphate regeneration.

Below this maximum layer, phosphate distributions differ considerably from crossing to crossing. A minimum in concentration was observed and is particularly pronounced on crossing 3 of Section C, with values near 1.1 μg-at l^{-1}.

In 1968, Paskausky and Nowlin constructed characteristic relationships between dissolved phosphate and preformed phosphate as functions of depth and dissolved-oxygen concentrations. These characteristic relations displayed wide limits of scatter indicating either that phosphate does not seem to be a good indicator of small scale current and water mass structures in the Gulf of Mexico or that the data used were not internally consistent. Only gross features of the current pattern are displayed in the phosphate vertical sections.

Section B, occupied on May 8, lies just to the south of Section C at a more east-west orientation. Station 26 is common to both sections. As seen in Fig. 1, Section B intersects the current at an angle more normal to the flow than does Section C. This section, occupied only once, does not extend completely across the inflowing Yucatan Current as may be seen in Fig. 8, which depicts distribution of dissolved oxygen, dissolved silicate, and dissolved phosphate as well as geostrophic speeds relative to the deepest observation depth on the section. Although some southward counterflow is seen at intermediate depths between Stations 25 and 26 on Section B, this section did not extend far enough to the west to show the extent of this southward flow.

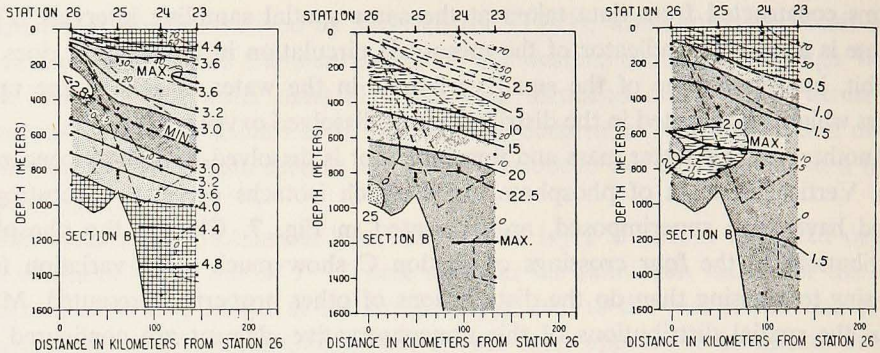

Figure 8. Vertical sections of dissolved oxygen (ml l^{-1}), dissolved silicate (μg-at l^{-1}), and dissolved phosphate (μg-at l^{-1}) for Section B. Superimposed are isotachs of relative geostrophic speed (cm sec^{-1}) normal to the section.

By way of contrast, Section A, which is parallel to Section B and located about 65 km to the south (see Fig. 12 for locations), extended westward to water depths of about 100 m. The vertical sections of dissolved-oxygen, dissolved-silicate, and dissolved-phosphate distributions, with superimposed relative geostrophic speeds, are presented in Fig. 9 for the two crossings of Section A, occupied May 7-8 and May 18. Significant differences between the two crossings of this section are seen in the thermohaline, oxygen, and nutrient distributions. On the first crossing (Stations 18-21), the isotachs of relative geostrophic speed indicate that the core of the current was about 75 km from the location of Station 18 with speeds approaching 150 cm sec^{-1}. The second crossing shows that the current core was located about 140 km from the position of Station 51 (or 18), and was east of the easternmost observations made on this crossing. The maximum geostrophic speeds estimated from crossing 2 were about 100 cm sec^{-1}, but these should not be taken as indicative of the current core speed. In addition, a weak countercurrent was apparent to the west of the main current of crossing 2, but no indication of such a current was seen on crossing 1. It appears that during the first crossing, this southward current was farther to the west than during the second crossing.

Slopes of oxygen isopleths are greater at depths of 200-600 m on the first crossing than on the second. In addition, the phosphate field shows a maximum core located 130 km from Station 18 on crossing 1, while it is against the continental slope on crossing 2. The slopes of silicate isopleths on both crossings again correspond closely to isotherms, with the first crossing having greater slopes than the second. At this section, the silicate maximum is found at approximately 1100-1200 m. It is likely that the current was so intense during crossing 1 that current-induced upwelling, as previously noted by Cochrane (1963, 1965, 1967, 1969), occurred.

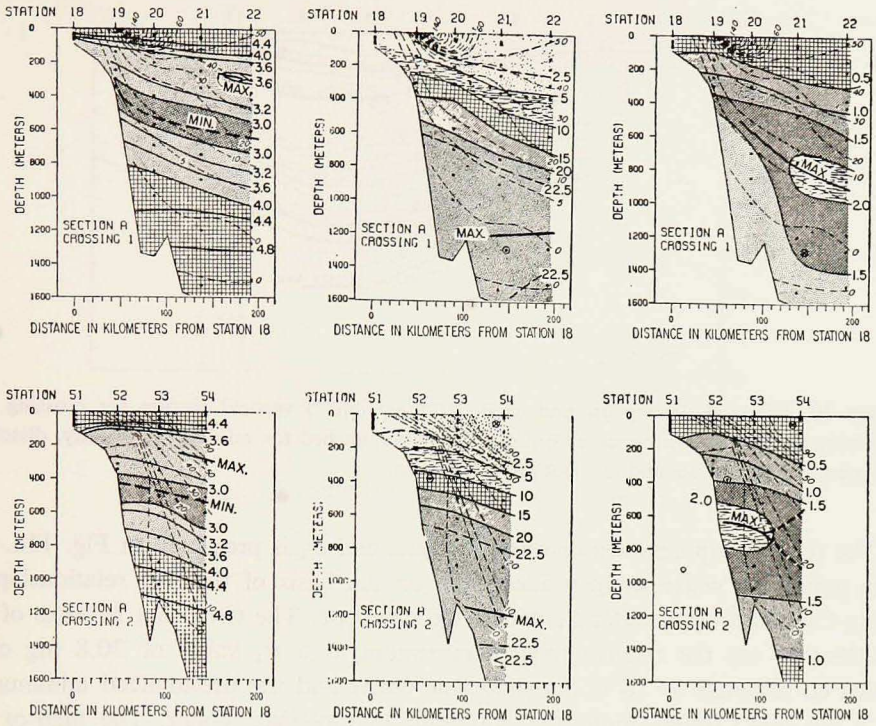

Figure 9. Vertical sections of dissolved oxygen (ml l^{-1}), dissolved silicate (μg-at l^{-1}), and dissolved phosphate (μg-at l^{-1}) for two crossings of Section A. Superimposed are isotachs of relative geostrophic speed (cm sec^{-1}) normal to the section.

3. Discussion

a. Systematic relationships. Dissolved oxygen, dissolved silicate, and dissolved phosphate were related to density on vertical sections for each crossing of the Loop Current made during Cruise 72-A-9. One such section is presented in Fig. 10. This section was constructed using the density parameter σ_0 from 0-1000 m and σ_1 from 500-1500 m. The parameter σ_0 or σ_1 was defined by Lynn and Reid (1968) by the relation $\sigma = (\rho - 1) \times 10^3$ where ρ is the density that a water parcel would have if moved adiabatically from its *in situ* position to the sea surface or 1000 decibars, respectively. Superimposed upon the density field are the positions of the principal water mass cores, as previously identified on vertical sections of oxygen and nutrients.

Another method of looking at the relationships between the density field and water masses is through the construction of scatter diagrams depicting nutrient or oxygen concentrations versus density parameters. For the density parameter σ_1, all data from *Alaminos* 72-A-9 are presented in scatter plots (Fig. 11) for the eastern Gulf of Mexico.

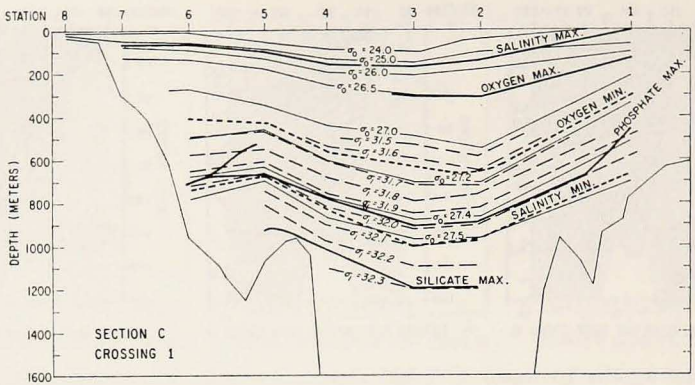

Figure 10. Potential density (σ_0 and σ_1 in 10^{-3} gm cm^{-3}) vertical section for crossing 1 at Section C. Also shown are cores (solid for maxima, dashed for minima) of salinity, dissolved-oxygen concentration, and nutrient concentrations.

The relationship between dissolved oxygen and σ_1 is presented in Fig. 11a. The data points for water samples identified, on the basis of the T-S relationship, as being Caribbean-type water lie within the envelope. The two main features of this relationship are the relative oxygen maximum at a σ_1 value of 30.8 mg cm^{-3} which corresponds to 18°C Sargasso Sea Water and the pronounced minimum at 31.7 mg cm^{-3} found above the Antarctic Intermediate Water. The high-oxygen values falling outside the envelope between 28 and 31 mg cm^{-3} correspond to those stations taken outside the Loop Current, e.g. in Gulf-type waters.

The silicate versus σ_1 relationship (Fig. 11b) has only one pronounced feature, a silicate maximum at approximately 32.3 mg cm^{-3}. This maximum corresponds to the remnant of Antarctic Intermediate Water found in the Gulf. The phosphate versus σ_1 relationship (Fig. 11c) shows a pronounced phosphate maximum near $\sigma_1 = 31.9$ mg cm^{-3}. Although positioned somewhat above the silicate maximum, this phosphate extremum is also associated with the Intermediate Water. The scatter in phosphate concentrations as seen in this diagram is presumably due at least in part to local effects.

Summarized in Table 1 are the relationships of nutrients and dissolved oxygen to density and water masses. Included in this table are the silicate minimum at $\sigma_0 = 27.80$ mg cm^{-3} and the phosphate minimum at $\sigma_0 = 27.85$ mg cm^{-3} due to North Atlantic Deep Water (NADW) which are found in the equatorial Atlantic (Morrison, 1974), but do not reach the Gulf due to shallow sill depths. Note that the "cores" of different tracers may be found at slightly different depths or densities although associated with a single source water mass.

The dissolved-oxygen and nutrient distributions seem to be good water mass tracers and closely tied to the flow regime in the eastern Gulf. In particular, dissolved oxygen reflects small scale variations in the current structure of the upper

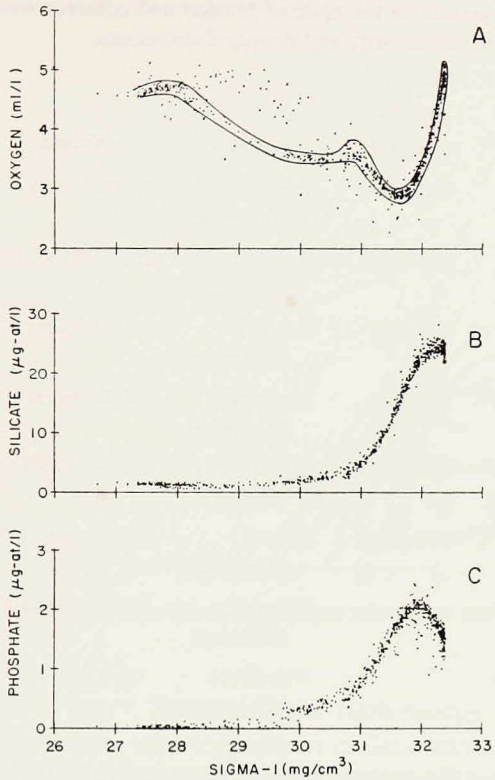

Figure 11. Scatter plots for all data from *Alaminos* 72-A-9 in southeastern Gulf of Mexico; potential density anomaly (σ_1 in 10^{-3} mg cm^{-3}) versus: (a) dissolved oxygen, (b) silicate, and (c) phosphate.

layers, and silicate is a sensitive indicator of the mesoscale circulation of the intermediate waters.

b. Currents and transports. We present the geopotential anomaly of the sea surface relative to 800 decibars (Fig. 12) in order to show the surface flow in the eastern Gulf during May, 1972. Only the Loop Current and a large anticyclonic ring are in evidence, though other features may have been present over the Campeche Bank and northeastern Gulf shelves.

The dynamic method also was used to calculate the geostrophic transports across each section (Table 2). Once again the deepest observed depth on each section was used as the reference level for the transports. Excluding the value for crossing 2 of Section A, which did not extend completely across the northward flow, the average transport value obtained from six crossings of the Yucatan Current is $30 \times 10^6 m^3 sec^{-1}$. Transports in the southward flowing limb of the Loop and in the

Table 1. Water masses present in the Gulf of Mexico and adjacent western regions as related to particular features in the property and density distributions.

σ_0 mg cm^{-3}	σ_1 mg cm^{-3}	Depth Range (meters)	Feature	Values	Water Mass
25.40	30.70	150-250	Salinity Maximum	36.70-36.80‰	SUW
26.50	30.80	200-400	Oxygen Maximum	3.60-3.80 ml l^{-1}	18°C Sargasso Sea Water
27.15	31.65	400-700	Oxygen Minimum	2.85-3.25 ml l^{-1}	
27.40	31.95	700-900	Phosphate Maximum	1.8-2.5 μg-at l^{-1}	AAIW
27.50	32.10	800-1000	Salinity Minimum	34.88-34.89‰	AAIW
27.70	32.30	900-1200	Silicate Maximum	23-25 μg-at l^{-1}	AAIW
27.80	32.40		Silicate Minimum	15-20 μg-at l^{-1}	NADW
27.85	33.00		Phosphate Minimum	1.2-1.3 μg-at l^{-1}	NADW

southward flow along the eastern edge of Campeche Bank also are tabulated for appropriate crossings.

Though the transport values given here are not directly comparable with other estimates because of the special manner in which a reference was selected, our estimates are not greatly different from previous estimates of Loop Current transport. Based on data from the summers of 1966 and 1967, Nowlin and Hubertz (1972) found the baroclinic, geostrophic transport within the upper 1350 decibars

Table 2. Geostrophic transports, in units of 10^6m^{3}sec^{-1}, calculated for sections across the current using the deepest observation as the reference surface.

Section	Crossing	Total Northward Flow	Total Southward Flow	Western Counter Flow	Northward Flow Above $\sigma_t = 27.0$
A	1	29.8			24.8
	2	17.5		0.4	
B		27.7		0.2	22.2
C	1	33.2	35.3	2.5	29.2
	2	34.8		4.1	24.5
	3	25.8			21.0
	4	31.0		5.9	22.1

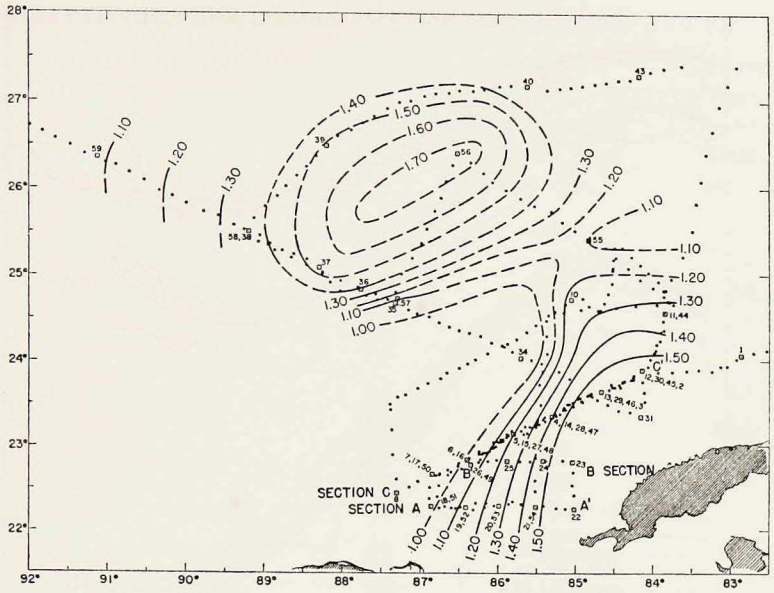

Figure 12. Geopotential anomaly (dyn m) of sea surface relative to 800 db surface constructed from *Alaminos* 72-A-9 data.

to be at least 30 × 10^6m^{3}sec^{-1}. Relative to the 1000-decibar surface, Nowlin and McLellan (1967) estimated the volume transport in the outflowing limb of the Loop to be 30 × 10^6m^{3}sec^{-1}. Based on three detailed hydrographic sections across the inflowing Yucatan Current in April, 1970, Schlitz (1973) estimated the net northward transport in the Yucatan Current relative to the deepest observed depth to be 27 × 10^6m^{3}sec^{-1}. Based on his estimate that waters with temperatures less than 5.5°C entering the Gulf cannot exit through the Florida Straits, Schlitz adjusted the transport through the Yucatan Strait so that there was no net transport below 5.5°C and found an average net northward transport of 30.5 × 10^6m^{3}sec^{-1} above that isotherm. Using dropsondes to measure transports, Schmitz and Richardson (1968) obtained a transport of 29.6 × 10^6m^{3}sec^{-1} entering the Florida Straits from the Loop Current.

During the same period of our measurements, sixteen dropsonde cross-sections were made across the Florida Straits south of Key West, Florida from the R. V. *Gulf Stream*. The measured transports for thirteen of those sections were reported by Brooks and Niiler (1975). The average transport from the surface down to the 27.0 σ_t contour was 21.4 × 10^6m^{3}sec^{-1} with a standard deviation of 2.3 × 10^6m^{3}sec^{-1}. For comparison, we have calculated the geostrophic transport, relative to the greatest observed depth, from the surface to the 27.0 σ_t contour for six crossings of the Yucatan Current. The average of these values (presented in Table 2) is 24.2 × 10^6m^{3}sec^{-1}. Also during May, 1972, multiple crossings of the Yucatan

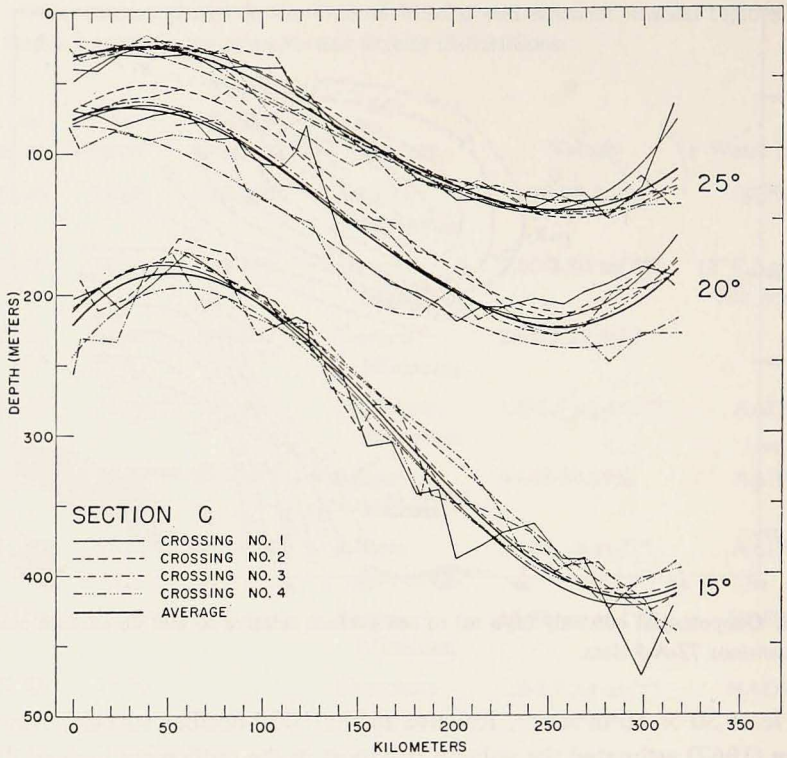

Figure 13. Isotherm depths of 25°, 20°, and 15°C isotherms for four crossings of Section C. Also shown are least square fits, using third-degree polynomial, for each isotherm.

Strait were made between Isla Mujeres, Mexico and Cabo San Antonio, Cuba, using a ship and airplane, with the objective of studying the inflow of the Yucatan Current. Using direct surface current measurements as the reference, geostrophic transports between the surface and the 27.0 σ_t contour were made by Molinari and Yager (1977). The average transport estimate obtained is 22.3 $\times$ $10^6 m^3 sec^{-1}$. This agreement is remarkable when one considers that the transports calculated for the two Straits may be low, since those sections stopped about 35 km from Cuba and probably do not capture the entire flow. These values yield an average transport between the surface and σ_t = 27.0 mg cm^{-3} of approximately 23 $\times$ $10^6 m^3 sec^{-1}$ for the Loop Current during May, 1972.

c. Variability in thermal structure. To obtain a closer look at the small-scale variations of the Loop Current, close analysis was made of the temperature structure observed with XBT's. Fig. 13 shows the thermal structure of the four crossings of Section C. These sections show considerable variation in the depths of isotherms. An attempt has been made to quantify these variations and to obtain the best mean pattern based on the four crossings.

Table 3. Data from computer-fit isotherms for 4 crossings of Section C.

Isotherm °C	Crossing	Maximum Slope (10^{-3})	Distance (km) of Max. Slope from Sta. 7	Average Difference (m) from the Average Isotherm
25°	1	1.4	140	6.6
	2	1.3	150	0.1
	3	1.0	130	2.0
	4	1.2	140	−5.8
	Average	1.1	150	
20°	1	1.6	160	6.3
	2	1.6	170	14.1
	3	1.5	170	3.6
	4	1.5	160	−22.6
	Average	1.5	160	
15°	1	2.2	175	−1.6
	2	2.2	175	4.5
	3	1.8	185	8.8
	4	1.9	185	−3.3
	Average	2.1	185	

The depths of the 25°, 20°, and 15°C isotherms were tabulated for each of the four crossings; third-degree polynomials were fit to these data using the method of least squares (polynomials of higher order did not improve the fit); and correlation coefficients were calculated. The correlation coefficients for the fits of individual crossings were .95 or better. An average curve for all four crossings was also generated. These fitted curves together with the observed isotherm depths are shown in Fig. 13. Table 3 contains the maximum isotherm slopes, the distance of the position of these slopes from the position of Station 7 for each crossing, and the average difference between the computer fitted isotherms for each crossing and the average isotherm for the section. The slopes of these fitted isotherms may be compared with estimates by Cochrane (1961) for the current downstream of the Yucatan Strait. Cochrane gives a maximum slope of the 20° isotherm of 2.0×10^{-3}, while the maximum slope of the 20° isotherm along Section C is $1.5\text{-}1.6 \times 10^{-3}$.

Lateral speeds were also calculated for the current using these data. The times from the middle of one crossing to the middle of the next were used, together with the distance that the position of maximum slope (current core) changed for the 25°C isotherm, to give lateral speeds of about 3 cm sec^{-1} eastward between crossings 1 and 2, 8 cm sec^{-1} westward between crossings 2 and 3, and 1 cm sec^{-1} eastward between crossings 3 and 4 for an average lateral speed of 4 cm sec^{-1}. The

15° isotherm shows a different tendency. The lateral speeds at this level are 2 cm sec^{-1} eastward, between crossings 1 and 2, 6 cm sec^{-1} eastward between crossings 2 and 3, and 3 cm sec^{-1} westward between crossings 3 and 4 for an average lateral speed of 4 cm sec^{-1}. Note that the direction of lateral shift of the upper waters differs from that of the deeper waters.

These estimates of the lateral movements of the Loop give a rough idea of its scales of variability. Many estimates of variability of the current system downstream of the eastern Gulf are available. Robinson *et al.* (1974) give typical values for the small scale variations of the Gulf Stream on the order of 20-30 km at velocities of 5 ± 2 cm sec^{-1} with a time scale of 3 ± 1 days. Mooers and Brooks (1973) found fluctuations in the temperature field within the Florida Straits that had periods of 4-5 days. Also, the work of Kielmann and Düing (1974), within the Florida Straits, shows typical fluctuations in the range of 5-6 days.

Possibly a more concise picture of the variability of the Loop within the open Gulf may be constructed when the remainder of the data from the 1972 field program is correlated with those data presented here. Then, changes in velocity and transport of the current as it enters and leaves the Gulf may be related to the changes within the Gulf.

4. Summary

The circulation regime of the eastern Gulf of Mexico during May 1972 was described using maps of both the geopotential anomaly and thermal fields. The Loop Current, entering the Gulf through Yucatan Straits, was observed to penetrate only as far north as 25°N. A large anticyclonic ring, with radius of at least 200 km, is known to have separated from the Loop during April and was centered at approximately 26° 30′ N and 87°W. During May, some development of the gross circulation pattern was occurring, but the variability was not great on the basis of the time sequence of three charts showing the depth of the 22°C isotherm. However, considerable small scale variability was present as evidenced by the comparison of repeated temperature sections across the Loop Current at Section C which was centered at approximately 23°N.

The distribution of salinity, dissolved oxygen, phosphate, and silicate along sections spanning the Loop Current allowed us to relate these parameters to Gulf-type and Caribbean-type waters. Within the eastern Gulf of Mexico, the various water masses present were identified and related to potential density surfaces. In particular, the values of the potential density parameter σ_0 and the associated water mass cores were: 25.40 mg cm^{-3}-Subtropical Underwater (salinity maximum), 26.50 mg cm^{-3}-18°C Sargasso Sea Water (oxygen maximum), 27.15 mg cm^{-3}-upper subtropical oxygen minimum, 27.40 mg cm^{-3}-Antarctic Intermediate Water (phosphate maximum), 27.50 mg cm^{-3}-Antarctic Intermediate Water (salinity minimum) and 27.70 mg cm^{-3}-Antarctic Intermediate Water (silicate maximum). Based on

this information, the observed distributions of characteristics were related to the water masses present and to the geostrophic current regime.

The measurements were also used to calculate the relative geostrophic transport through six sections across the current. The average transport during May was 30 $\times$ 10 $m^6 sec^{-1}$. This estimate compared favorably with published estimates for the Loop Current. In addition, we estimated the transport above the 27.0 mg cm^{-3} σ_t surface to be 23 $\times$ $16^6 m^3 sec^{-1}$ which agrees quite well with values obtained during the same time period by other workers at the Yucatan and Florida Straits.

Acknowledgments. This work was supported by the Office of Naval Research under contract N00014-75-C-0259. The funds for *Alaminos* cruise 72-A-9 were provided by the National Science Foundation under Contract GD 31790. We wish to express our appreciation to Dr. William J. Merrell, Jr., who made preparations for cruise 72-A-9 and was scientist-in-charge aboard *Alaminos;* to Mrs. Ruth A. McMath, who aided us in the computer reduction and presentation of these data; and to Mr. Oscar Chancey, who prepared the final figures presented in this paper.

REFERENCES

Atlas, E., L. Gordon, S. Hager, and P. K. Park. 1971. A practical manual for the use of the Technicon Auto-analyzer in sea water nutrient analysis: revised. Unpubl. Tech. Rept. 215 of Dept. of Oceanogr., Oregon State Univ., Ref. 71-22, 35 pp.

Brooks, I. H., and P. P. Niiler. 1975. The Florida Current at Key West: Summer 1972. J. Mar. Res., *33*, 83–92.

Cochrane, J. D. 1961. Investigations of the Yucatan Current. Unpubl. Tech. Rept. of Dept. of Oceanogr., Texas A&M Univ., Ref. 61-15F, 4–7.

—— 1963. Yucatan Current. Unpubl. Tech. Rept. of Dept. of Oceanogr., Texas A&M Univ., Ref. 63-18A, 6–11.

—— 1965. The Yucatan Current and equatorial currents of the western Atlantic. Unpubl. Tech. Rept. of Dept. of Oceanogr., Texas A&M Univ., Ref. 65-17T, 6–27.

—— 1967. Upwelling off northeast Yucatan. Unpubl. Tech. Rept. of Dept. of Oceanogr., Texas A&M Univ., Ref. 67-11T, 16–17.

—— 1969. Water and circulation on Campeche Bank in May. Bull. Jap. Soc. Fisheries Oceanogr., Special Number (Prof. Uda's Commemorative Papers), 123–128.

Corcoran, E. F. 1973. Chemical Oceanography, *in* A Summary of Knowledge of the Eastern Gulf of Mexico 1973. State Univ. System of Florida Institute of Oceanography, St. Petersburg, Florida.

Fomin, L. M. 1964. The Dynamic Method in Oceanography. New York, Elsevier Publishing Company, 212 pp.

Kielmann, J. and W. Düing. 1974. Tidal and sub-inertial fluctuations in the Florida Current. J. Phys. Oceanogr., *4*, 227–236.

Kinard, W. F., D. K. Atwood, and G. S. Giese. 1974. Dissolved oxygen as evidence for 18°C Sargasso Sea water in the eastern Caribbean Sea. Deep-Sea Res., *21*, 79–82.

Lynn, R. J., and J. L. Reid. 1968. Characteristics and circulation of deep and abyssal waters. Deep-Sea Res., *15*, 577–598.

Molinari, R. L. 1967. The effect of topography on the Yucatan Current. Unpubl. Tech. Rept. of Dept. of Oceanogr., Texas A&M Univ., Ref. 67-24T, 49 pp.

Molinari, R. L., and R. Yager. 1977. Upper layer hydrographic conditions at the Yucatan Strait during May 1972. J. Mar. Res., *35*, this issue.

Mooers, C. N. K., and D. A. Brooks. 1973. Several-day to several-week fluctuations in the Florida Current (abstract). Trans. Amer. Geophys. Union, *54*, 311.

Morrison, J. M. 1974. Nutrient and dissolved oxygen distributions in the Gulf of Mexico and adjacent regions. Unpublished Masters thesis, Texas A&M University.

Morrison, J. M., W. Merrell, and W. D. Nowlin, Jr. 1973. The waters of the eastern Gulf of Mexico as observed during May 1972; I. Data collected aboard the R. V. *Alaminos*. Unpubl. Tech. Rept. of Dept. of Oceanogr., Texas A&M Univ., Ref. 73-10T, 330 pp.

Nowlin, W. D., Jr., and J. M. Hubertz. 1972. Contrasting summer circulation patterns for the eastern Gulf-Loop Current versus anticyclonic ring, *in*, Contributions on the Physical Oceanography of the Gulf of Mexico. Capurro, L. R. A. and J. L. Reid, ed., *2*, 119–138.

Nowlin, W. D., Jr., and H. J. McLellan. 1967. A characterization of the Gulf of Mexico waters in winter. J. Mar. Res., *25*, 29–59.

Nowlin, W. D., Jr., D. F. Paskausky, and H. J. McLellan. 1969. Recent dissolved-oxygen measurements in the Gulf of Mexico deep waters. J. Mar. Res., *27*, 39–44.

Paskausky, D. F., and W. D. Nowlin, Jr. 1968. Measured and preformed phosphate in the Gulf of Mexico region. Unpubl. Tech. Rept. of Dept. of Oceanogr., Texas A&M Univ., Ref. 68-12T, 19 pp.

Redfield, A. C., B. H. Ketchum, and F. A. Richards. 1963. The influence of organisms on the composition of sea water, *in* The Sea. M. N. Hill, ed., vol. 2, New York, John Wiley & Sons, 554 pp.

Riley, G. A. 1937. The significance of the Mississippi River drainage for biological conditions in the northern Gulf of Mexico. J. Mar. Res., *1*, 60–74.

Robinson, A. R., J. R. Luyten, and F. C. Fuglister. 1974. Transient Gulf Stream meandering. Part I: An observational experiment. J. Phys. Oceanogr., *4*, 237–255.

Schlitz, R. J. 1973. Net total transport and net transport by water mass categories for Yucatan Channel, based on data for April 1970. Unpublished Ph.D. dissertation, Texas A&M University, 107 pp.

Schmitz, W. J., Jr., and W. S. Richardson. 1968. On the transport of the Florida Current. Deep-Sea Res., *15*, 679–694.

Wennekens, M. P. 1959. Water mass properties of the Straits of Florida and related waters. Bull. Mar. Sci. of Gulf and Caribbean, *9*, 1–52.

Worthington, L. V. 1959. The 18° water in the Sargasso Sea. Deep-Sea Res., *5*, 297–305.

Wüst, G. 1964. Stratification and circulation in the Antillean-Caribbean Basins. Part One. Spreading and mixing of the water types with an oceanographic atlas. Vema Research Series No. 2, Columbia University Press, New York, 201 pp.

Received: *13 February, 1976;* revised: *19 August, 1976.*